Dual-Mode Silicon Ring Resonator Based on Subwavelength Grating Directional Couplers

Mengyuan Ye, Yunlong Li, Zhepei Chen, Lijun Zhang, Li Liu, and Yu Yu, *Member, IEEE*

***Abstract*—We propose and experimentally demonstrate a dual-mode silicon ring resonator which could process TE_0 and TE_1 modes simultaneously. By introducing subwavelength grating into the coupling region, compact footprint of $\sim$90 μm $\times$ 20 μm is achieved. The proposed device is fabricated on the standard silicon-on-insulator platform. The measured results indicate the mode crosstalk within C band are less than $-$12.2 and $-$11.5 dB for TE_0 and TE_1 modes, respectively. Furthermore, heaters for resonant wavelength tuning are fabricated and measured with good uniformity for both modes.**

***Index Terms*—Mode multiplexing, subwavelength grating, silicon ring resonator.**

I. Introduction

In THE past decade, silicon photonics is commonly regarded as a promising solution for inter/intra data-center connections due to its advantages as low-cost, small footprint and compatibility with matured Complementary Metal-Oxide Semiconductor (CMOS) technology [1], [2]. To meet the increasing capacity requirement of optical interconnection, multiplexing technologies such as the wavelength division multiplexing (WDM), polarization division multiplexing (PDM) are intensively utilized [3], [4], [5], [6]. Nowadays, mode division multiplexing (MDM) technology attracts more and more attention due to its compatibility with other multiplexing technologies and ability on further increasing the transmission capacity [7]. In order to build a chip-level MDM network, a variety of fundamental building blocks, including mode multiplexer [8], multi-mode crossing [9], coupler [10], [11], [12], [13], have been extensively investigated. Advanced circuits, such as multi-mode switch and router, are further proposed and demonstrated [14], [15].

Due to the severe mode dispersion in silicon multimode waveguides, demultiplexing-process-multiplexing architecture is commonly used for MDM signal processing, resulting in a high-loss and inefficient layout. Recently, a novel multi-mode signal processing architecture attracts more and more attention for its ability on processing MDM signals simultaneously [16], [17]. Thus, MDM signal processing circuits with high performance and small footprint could be achieved.

Micro-ring resonator (MRR) as an essential element in silicon integrated circuit, is widely utilized as filter [18], modulator [19] and sensor [20] in single-mode regime. With the development of MDM technology, MRR that could process multi-mode signals is highly desired. However, it is difficult to achieve a multi-mode MRR with compact footprint, due to the severe mode dispersion in the coupling region. Reported MRR [21] used a conventional directional coupler to achieve uniform two-mode coupling with a racetrack length of 95 μm, resulting an inefficient layout. MRR based on free space geometric optics [22] could overcome the mode dispersion and support more modes. However low Q-factor limits its application in practical system.

In this paper, we propose and experimentally demonstrate a dual-mode MRR with compact footprint. By introducing subwavelength grating [23] into the coupling region, length of the racetrack is reduced to 20 μm. The proposed device is fabricated on the standard silicon-on-insulator (SOI) platform. The measured results indicate the mode crosstalk within C band are less than -12.2 and -11.5 dB for TE_0 and TE_1 modes, respectively. Furthermore, heaters for resonant wavelength tuning are measured with good uniformity for both modes.

II. Design and Simulation

The scheme of the proposed device is shown in Fig. 1(a). The device consists of two 180° bends and two coupling regions. TE_0 and TE_1 modes at resonance wavelengths are coupled into the MRR through the input port and coupled out at the drop port. Coupling regions are designed as the SWG waveguides, which could enhance the coupling efficiency to realize compact coupling length. Bend radius is designed as 45 μm to support TE_0 and TE_1 modes transmission with low crosstalk. Thus, uniform process on TE_0 and TE_1 modes could be achieved. Design details of the SWG waveguides and multi-mode bends are introduced in following sections.

A. Subwavelength Grating Directional Coupler

Fig. 1(b) shows the top view of the proposed SWG waveguide. W represents the waveguide width. In order to support transmission of both TE_0 and TE_1 modes, W is chosen to be 1 μm. While Λ and η stand for the period and duty cycle of the subwavelength structure. To realize sufficient coupling for both

Manuscript received 8 June 2022; revised 16 August 2022; accepted 18 August 2022. Date of publication 22 August 2022; date of current version 31 August 2022. This work was supported by the National Natural Science Foundation of China under Grants 61911530161and 62175220. *(Corresponding author: Li Liu.)*

Mengyuan Ye, Yunlong Li, Zhepei Chen, Lijun Zhang, and Li Liu are with the School of Automation and Hubei Key Laboratory of Advanced Control and Intelligent Automation for Complex Systems, China University of Geosciences, Wuhan 430074, China (e-mail: yemy@cug.edu.cn; liyunlong@cug.edu.cn; chenzp@cug.edu.cn; zlj599@126.com; liliu@cug.edu.cn).

Yu Yu is with the Wuhan National Laboratory for Optoelectronics, Huazhong University of Science and Technology, Wuhan 430074, China (e-mail: yuyu@mail.hust.edu.cn).

Digital Object Identifier 10.1109/JPHOT.2022.3200690

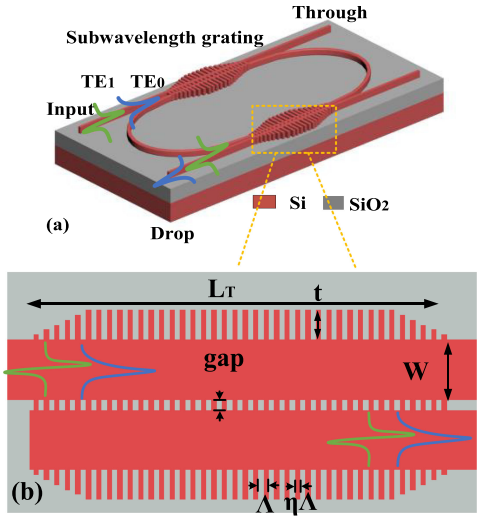

Fig. 1. (a) Schematic of the proposed mode-insensitive MRR; (b) Top view of the SWG waveguides.

TE_0 and TE_1 modes, Λ and η need to be carefully designed to meet both the SWG working condition and fabrication rules.

According to the equivalent dielectric theory [24], SWG waveguide could be regarded as a uniform equivalent dielectric material. The equivalent refractive index n_{eq} is given by

$$n_{eq}^2 = \eta \cdot n_{si}^2 + (1-\eta) \cdot n_{sio_2}^2 \tag{1}$$

n_{si} and n_{sio_2} are the refractive indices of the silicon and silica. To meet the SWG working condition [24], the period Λ needs to be designed as

$$\Lambda < \lambda_{\min}/(2 \cdot n_{eq}) \tag{2}$$

$\lambda_{\min}$ stands for minimum operating wavelength. To make the device work within C band, Λ and η are chosen as 280 nm and 0.5, respectively. Coupling gap is chosen as 220 nm. Furthermore, a SWG based taper with width of 600 nm and length of 1.4 μm is introduced to realize adiabatic mode coupling between channel waveguide and SWG waveguide.

Fig. 2(a) shows the simulated coupling efficiencies with different coupling length at 1550 nm for TE_0 and TE_1 modes. To achieve uniform light coupling for dual-mode signal process, coupling length is chosen to be 20 μm. Insertion losses of TE_0 and TE_1 modes are simulated to be ~0.26 dB and 0.4 dB, respectively. While mode crosstalk is simulated as ~-18 dB for both TE_0-TE_1 and TE_1-TE_0. The simulated light propagating evolution in SWG waveguides are shown in Fig. 2(b) and (c). To be noted, resonance of the mode field is caused by the Bloch-Floquet modes of the SWG structure [25], which could be reduced by selecting a smaller Λ.

B. Bend Waveguide

In order to reduce the mode crosstalk between TE_0 and TE_1 modes, arc waveguides with radius of 45 μm is usually used to form the dual-mode bends. Simulated transmission spectra of the bends are shown in Fig. 3(a), (b) and (c) illustrate the simulated light propagation for TE_0 and TE_1 modes.

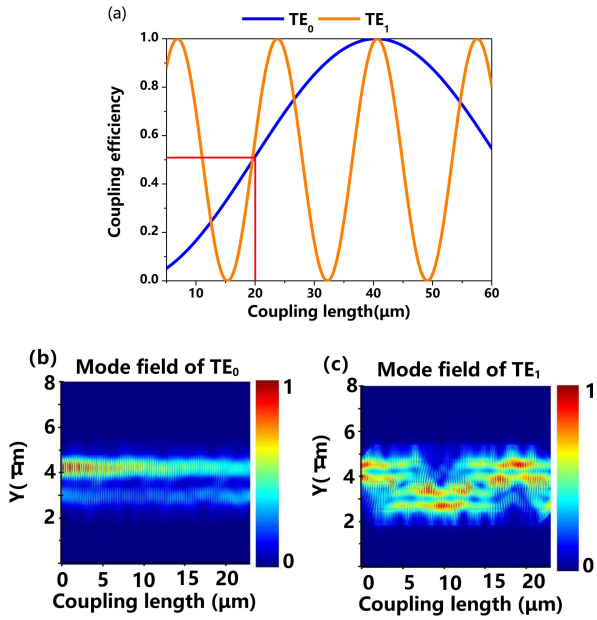

Fig. 2. (a) Simulated coupling efficiencies with different coupling length at 1550 nm for TE_0 and TE_1 modes and the light propagating evolution in the proposed SWG waveguides for (b) TE_0 and (c) TE_1 modes.

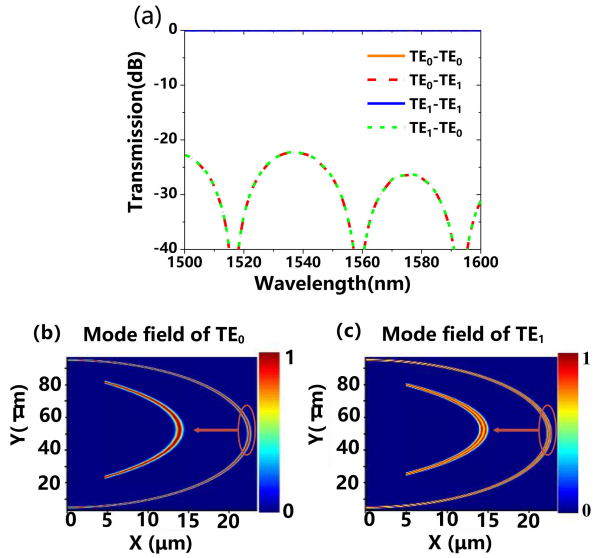

Fig. 3. (a) Simulated transmission spectra of the bent waveguide for TE_0 and TE_1 modes. Simulated light propagation for (b) TE_0 and (c) TE_1 modes.

In the legend "TE_0-TE_1", the first "0" stands for the input TE_0 mode, while the second "1" stands for the output TE_1 mode. Results indicate insertion loss for TE_0 and TE_1 modes are~0.01 and 0.05 dB, respectively. While the mode crosstalk between TE_0 and TE_1 modes are<-22.2 dB within the C band.

C. Dual-Mode Ring Resonator

Combining the two key elements discussed above, the dual-mode MRR can be formed. In order to characterize the proposed device, the drop port transmission spectra for TE_0 and TE_1 modes are further simulated, as shown in Fig. 4. The simulation

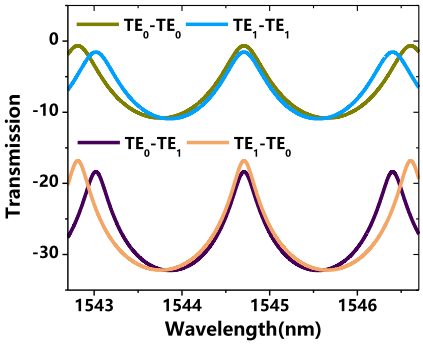

Fig. 4. Simulated the drop port transmission spectra of the proposed MRR for TE_0 and TE_1 modes.

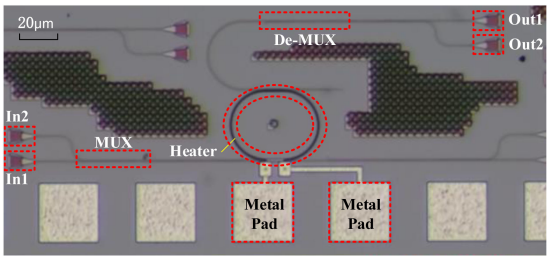

Fig. 5. Microscope image of the fabricated device.

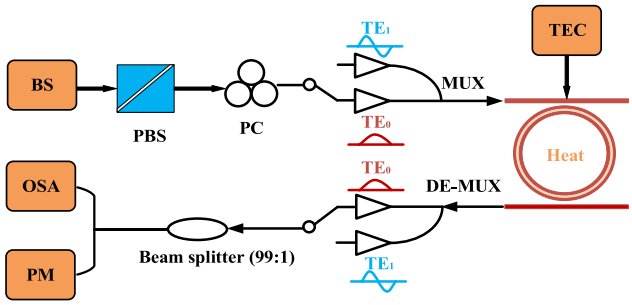

Fig. 6. The experiment setup.

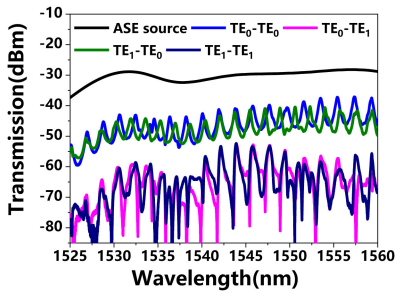

Fig. 7. Measured transmission spectra of the MRR for TE_0 and TE_1 modes input from 1530 to 1565 nm.

results indicate that bandpass filtering for dual-mode signals is successfully achieved. The insertion loss for TE_0 and TE_1 modes are simulated to be ~0.67 and 1.58 dB. While the mode crosstalk are ~-17.7 and -15.3 dB for TE_0 and TE_1 modes, respectively. Free spectrum ranges (FSRs) for TE_0 and TE_1 modes are simulated to be 1.9 and 1.7 nm. This can be increased by optimizing the bent waveguide to reduce its size.

III. Fabrication

The proposed device is fabricated on a SOI wafer with a 220 nm-thick top-silicon layer and SiO_2 buried layer of 2 μm. Fig. 5 shows the microscope image of the fabricated device. 248 nm deep ultraviolet photolithography and inductively coupled plasma (ICP) etching are used to form the waveguide structure. To form the channel waveguide, full etching is adopted. The waveguide width is chosen to be 1 μm to support dual-mode transmission. Λ and η of the SWG waveguide are chosen as 280 nm and 0.5, respectively. To achieve uniform dual-mode processing, coupling length and gap of the SWG coupling region are set as 20 μm and 220 nm. Furthermore, an adiabatic taper with width of 600 nm and length of 1.4 μm was introduced to realize adiabatic mode coupling between channel waveguide and SWG waveguide. The bending radius of the MRR is set to be 45 μm. In order to adjust the resonance wavelength of the ring, an integrated TiN heater is fabricated on top of the ring. The thickness and the width of the heater are 200 nm and 5 μm, respectively. The grating couplers (GCs) are used to couple light into and out of the chip. The circuit is fabricated at the Advanced Micro Foundry (AMF) in Singapore. Footprint of the fabricated MRR is 90 μm $\times$ 20 μm. In order to test the proposed MRR, adiabatic mode MUX and De-MUX are adopted. The insertion losses for TE_0-TE_1 modes are ~1.15 and 1.18 dB, respectively, and the mode crosstalk is ~-16 dB in the wavelength range of 1530–1565 nm.

IV. Measurement

The experiment setup is shown in Fig. 6. In order to verify the performance of the fabricated device, the transmission spectra over C band of the fabricated device is measured, by introducing the light from a broadband source (BS). Assisting by the polarization beam splitter (PBS) and polarization controller (PC), linearly polarized light input can be achieved. The chip is set on the coupling test platform. With the help of Thermo Electric Cooler (TEC), temperature of the test environment is kept at 25±0.01°C. On-chip heater is used to tune the resonance wavelength for both TE_0 and TE_1 modes. A fiber based beam splitter is utilized to split 1% of the output light into power meter (PM) for power monitoring, and 99% of the output light is launched into the optical spectrum analyzer (OSA) for transmission spectra measurement. The light input from port In_1 stands for the input TE_0 mode. The transmission spectrum of TE_0 is measured at port Out1, and the crosstalk is measured at port Out2. Details of the measured results are demonstrated and discussed in the following section.

V. Results and Discussion

Transmission spectra within C band for TE_0 and TE_1 modes are measured. The results are shown in Fig. 7.

The total losses of the fabricated circuit for TE_0 and TE_1 modes are measured to be 13 and 14.73 dB. Coupling loss of the grating coupler fabricated on the same chip is measured to

TABLE I
THE SIMULATION AND EXPERIMENT RESULTS

FOM	ER(dB)		FSR(nm)		Crosstalk(dB)		Q factor	
Mode	TE_0	TE_1	TE_0	TE_1	TE_0	TE_1	TE_0	TE_1
Simulation	10.2	9.4	1.9	1.7	-17.7	-15.3	3860	7644
Experiment	9.4	8.3	1.912	1.704	-12.1	-10.3	3300	5400

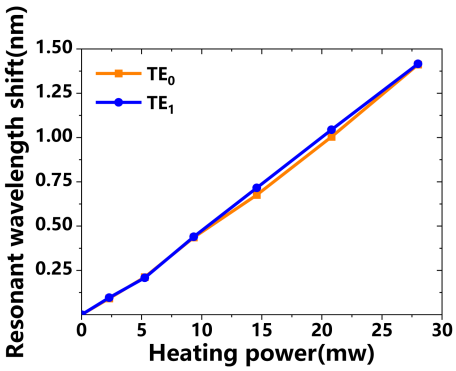

Fig. 8. Measured resonant wavelength shift with heating power from 0 to 28 mw for TE_0 and TE_1 modes.

be ∼5 dB. Thus the insertion losses of the fabricated MRR are ∼ 3 and 4.73 dB for TE_0 and TE_1 modes, respectively. The FSRs for TE_0 and TE_1 modes are measured to be 1.912 and 1.704 nm. The quality factors (Q-factors) for TE_0 and TE_1 modes are measured to be ∼3300 and 5400, respectively. The crosstalk for TE_0 and TE_1 modes are measured to be <-12.1 and -10.3 dB. To be noted, relatively low extinction ratio (∼8.3 dB) is due to the strong coupling in SWG waveguides, which could be improved by selecting a suitable coupling gap.

To make a clear comparison of the figure of merit (FOM) between simulation and experiment results. Extinction ratio (ER), FSR and crosstalk for TE_0 and TE_1 modes are collected and shown in Table I. The results indicate good consistency between simulation and measurement. Furthermore, uniformities of these FOMs indicate good performance of the proposed dual-mode signal processing. To be noted, the slight performance degradation is due to the imperfect fabrication process.

In order to adjust the resonance wavelength of the ring, an integrated TiN heater is fabricated on top of the MRR. To characterize the performance of the heater, resonant wavelength with different heating powers for TE_0 and TE_1 modes are measured respectively. The measured results are shown in Fig. 8. The tuning efficiency for TE_0 and TE_1 modes are measured to be 0.0504 and 0.0505 nm/mw, respectively.

VI. CONCLUSION

In summary, we propose and experimentally demonstrate a dual-mode silicon ring resonator which could process TE_0 and TE_1 modes simultaneously. By introducing subwavelength grating into the coupling region, compact footprint of ∼90 μm × 20 μm is achieved. Measured results show good multi-mode processing is successfully achieved. The proposed device could be utilized in advanced mode division multiplexing network.

REFERENCES

[1] D. Dai, "Advanced passive silicon photonic devices with asymmetric waveguide structures," *Proc. IEEE*, vol. 106, no. 12, pp. 2117–2143, Dec. 2018.
[2] W. Bogaerts and L. Chrostowski, "Silicon photonics circuit design: Methods, tools and challenges," *Laser Photon. Rev.*, vol. 12, no. 4, 2018, Art. no. 1700237.
[3] C. R. Doerr and T. F. Taunay, "Silicon photonics core-, wavelength-, and polarization-diversity receiver," *IEEE Photon. Technol. Lett.*, vol. 23, no. 9, pp. 597–599, May 2011.
[4] D. Dai and J. E. Bowers, "Silicon-based on-chip multiplexing technologies and devices for peta-bit optical interconnects," *Nanophotonics*, vol. 3, no. 4/5, pp. 283–311, 2014.
[5] K. Igarashi et al., "Ultra-dense spatial-division-multiplexed optical fiber transmission over 6-mode 19-core fibers," *Opt. Exp.*, vol. 24, no. 10, pp. 10213–10231, 2016.
[6] L. W. Luo et al., "WDM-compatible mode-division multiplexing on a silicon chip," *Nature Commun.*, vol. 5, no. 10, 2014, Art. no. 3069.
[7] D. J. Richardson, J. M. Fini, and L. E. Nelson, "Space-division multiplexing in optical fibres," *Nature Photon.*, vol. 7, no. 5, pp. 354–362, 2013.
[8] A. M. J. Koonen, H. Chen, H. P. A. van den Boom, and O. Raz, "Silicon photonic integrated mode multiplexer and demultiplexer," *IEEE Photon. Technol. Lett.*, vol. 24, no. 21, pp. 1961–1964, Nov. 2012.
[9] H. Chen, H. Hou, G. Wang, and H. Wang, "Novel design of multi-mode-interference crossings for periodic dielectric waveguides," *Opt. Commun.*, vol. 361, pp. 59–64, 2016.
[10] D. Dai, J. Wang, and S. He, "Silicon multimode photonic integrated devices for on-chip mode-division- multiplexed optical interconnects," *Prog. Electromagn. Res.*, vol. 143, pp. 773–819, 2013.
[11] D. Dai, "Multimode optical waveguide enabling microbends with low inter-mode crosstalk for mode-multiplexed optical interconnects," *Opt. Exp.*, vol. 22, no. 22, pp. 27524–27534, 2014.
[12] C. Sun, Y. Yu, G. Chen, and X. Zhang, "Ultra-compact bent multimode silicon waveguide with ultralow inter-mode crosstalk," *Opt. Lett.*, vol. 42, no. 15, pp. 3004–3007, 2017.
[13] X. Wu et al., "Low crosstalk bent multimode waveguide for on-chip mode-division multiplexing interconnects," in *Proc. CLEO: QELS_Fundam. Sci.*, 2018, pp. 1–2.
[14] H. Xiao et al., "Optical mode switch based on multimode interference couplers," *J. Opt.*, vol. 19, no. 2, 2017, Art. no. 025802.
[15] R. R. Patel et al., "Multi-mode fiber coarse WDM grating router using broadband add/drop filters for wavelength re-use," in *Proc. IEEE Lasers Electro-Opt. Soc.*, 1999, vol. 2, pp. 826–827.
[16] Y. Luo, Y. Yu, M. Ye, C. Sun, and X. Zhang, "Integrated dual-mode 3 dB power coupler based on tapered directional coupler," *Sci. Rep.*, vol. 6, no. 1, pp. 1–7, 2016.
[17] G. Zhang, H. R. Mojaver, A. Das, and O. Liboiron-Ladouceur, "Mode insensitive switch for on-chip interconnect mode division multiplexing systems," *Opt. Lett.*, vol. 45, pp. 811–814, 2020.
[18] H. Qiu et al., "A continuously tunable sub-gigahertz microwave photonic bandpass filter based on an ultra-high-Q silicon microring resonator," *J. Lightw. Technol.*, vol. 36, no. 19, pp. 4312–4318, 2018.
[19] B. Stern, X. Ji, A. Dutt, and M. Lipson, "Compact narrow-linewidth integrated laser based on a low-loss silicon nitride ring resonator," *Opt. Lett.*, vol. 42, no. 21, pp. 4541–4544, 2017.
[20] B. Su, C. Wang, Q. Kan, and H. Chen, "Compact silicon-on-insulator dual-microring resonator optimized for sensing," *J. Lightw. Technol.*, vol. 29, no. 10, pp. 1535–1541, May 2011.
[21] B. A. Dorin and W. N. Ye, "Two-mode division multiplexing in a silicon-on-insulator ring resonator," *Opt. Exp.*, vol. 22, no. 4, pp. 4547–4558, 2014.
[22] M. Ye, C. Sun, Y. Yu, Y. Ding, and X. Zhang, "Silicon integrated multi-mode ring resonator," *Nanophotonics*, vol. 10, no. 2, pp. 1265–1272, 2021.
[23] C. Ye and D. Dai, "Ultra-compact broadband 2 × 23 dB power splitter using a subwavelength-grating-assisted asymmetric directional coupler," *J. Lightw. Technol.*, vol. 38, no. 8, pp. 2370–2375, 2020.
[24] R. Halir et al., "Subwavelength-grating metamaterial structures for silicon photonic devices," *Proc. IEEE*, vol. 106, no. 12, pp. 2144–2157, Dec. 2018.
[25] J. D. Joannopoulos, S. G. Johnson, J. N. Winn, and R. D. Meade, "Symmetries and solid-state electromagnetism," in *Photonic Crystals*, 2nd ed. Princeton, NJ, USA: Princeton Univ. Press, 2008, pp. 25–43.